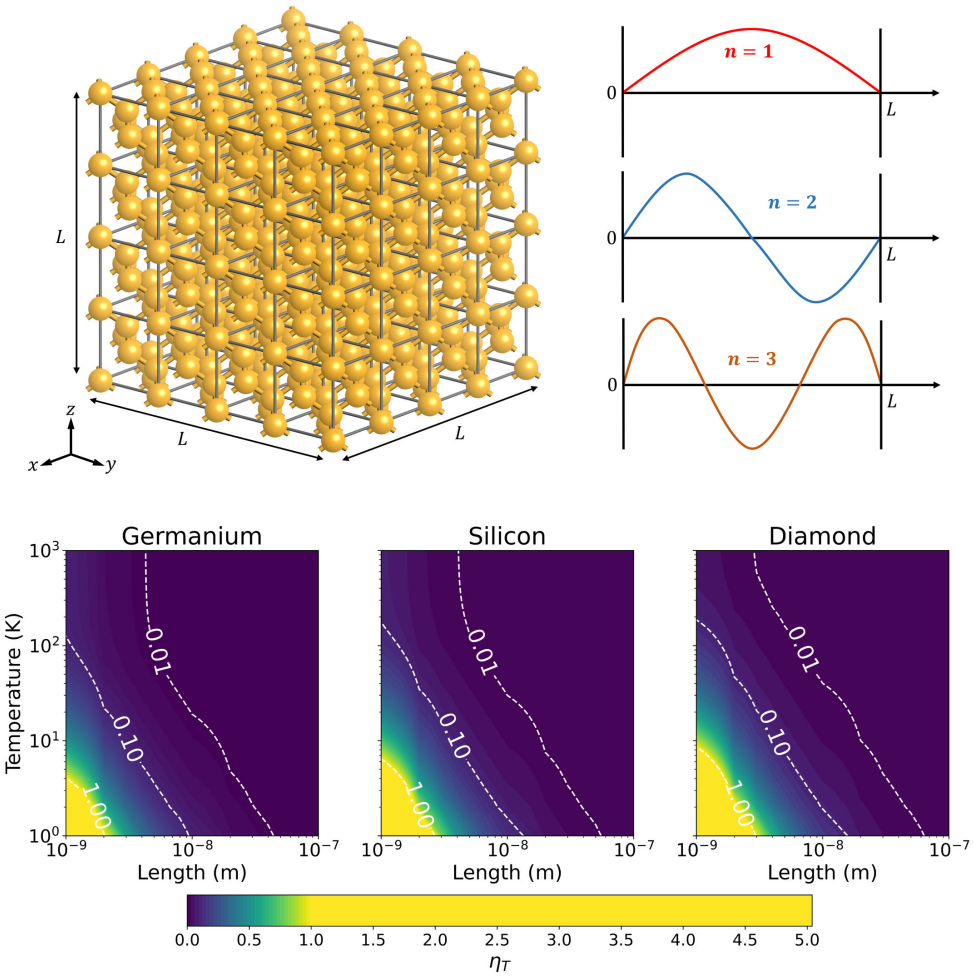


Graphical Abstract

Temperature Fluctuations in Quantum Dots: Insights from a $T^{3/2}$ Heat Capacity Model

Shixian Liu, Vladimir I. Khvesyuk



Temperature Fluctuations in Quantum Dots: Insights from a $T^{3/2}$ Heat Capacity Model

Shixian Liu^a, Vladimir I. Khvesyuk^{a,*}

^a*Department of Thermophysics, Bauman Moscow State Technical University, 2nd Baumanskaya 5, Moscow, 105005, Russian Federation*

Abstract

In this study, the temperature fluctuations in three-dimensional confined nanostructures (quantum dots) of germanium, silicon, and diamond were calculated using the $T^{3/2}$ model based on the particle-in-a-box (PIAB) approach and compared with the Debye T^3 model. The analysis focused on quantum dots with sizes ranging from 1 to 100 nm. According to the PIAB $T^{3/2}$ model, temperature fluctuations decrease as the temperature decreases, consistent with the principles of statistical physics. In contrast, the Debye T^3 model predicts an increase in temperature fluctuations with decreasing temperature, contradicting the principles of statistical physics. These results emphasize the significant impact of quantum confinement and highlight the limitations of the Debye T^3 model in describing nanoscale systems. Furthermore, distribution diagrams illustrating temperature fluctuations as functions of size and temperature were established for the first time. Based on these diagrams, clear boundaries were defined for the temperature and thermophysical property ranges where reliable predictions can be made.

Keywords: Temperature fluctuations, temperature, nanothermodynamics, quantum dots, particle-in-a-box model

*Corresponding author

Email address: 2636623@gmail.com (Vladimir I. Khvesyuk)

1. Introduction

Temperature and other thermophysical concepts are traditionally defined for systems with large numbers of particles [1]. However, at the nanoscale, where the number of particles is greatly reduced, conventional temperature definitions may not hold due to significant fluctuations in thermodynamic properties [2] [3]. These fluctuations pose challenges for reliable data acquisition, complicating accurate temperature determination [4–7].

As the size of nanostructures decreases, temperature fluctuations become more pronounced, significantly influencing their behavior [8]. This phenomenon necessitates the development of precise measurement techniques to accurately capture thermal behavior at the nanoscale. Recent research has focused on advancing temperature measurement methods to enhance data reliability [9–11]. According to statistical mechanics, temperature fluctuations are inversely related to heat capacity [4]. In other words, systems with higher heat capacity exhibit smaller temperature fluctuations. Consequently, at low temperatures or in small systems, temperature fluctuations become more significant.

The influence of quantum confinement on the heat capacity of quantum dots (QDs) has garnered significant attention. For instance, Novotny et al. experimentally investigated the unique heat capacity behavior of fine lead particles [12]. Theoretically, McNamara et al. developed a heat capacity model by replacing the integral in the Debye model with a summation over the wave vector components [13]. Additionally, Roslee et al. combined density functional theory (DFT) calculations with modifications to the Debye model, incorporating the particle-in-a-box (PIAB) framework to propose a new $T^{3/2}$ model [14].

The Debye T^3 model [15, 16] predicts that temperature fluctuations in nanoscale structures diverge at low temperatures, contradicting statistical physics, which asserts that temperature fluctuations should not exceed the temperature itself. In contrast, the PIAB $T^{3/2}$ model, validated by density functional theory (DFT) [14], provides results more consistent with statistical physics.

In this paper, we perform theoretical calculations to compare temperature fluctuations in QDs, examining the effects of temperature and size. Specifically, we investigate the limitations of the Debye T^3 model for nanoscale systems, which predicts diverging temperature fluctuations at low temperatures—an outcome inconsistent with statistical physics. In contrast, the

PIAB $T^{3/2}$ model aligns with statistical expectations and highlights the influence of quantum confinement on thermal properties. We mapped temperature fluctuations as functions of size and temperature and, based on various criteria, identified the ranges within which temperature and thermophysical properties are reliably defined. This study provides new insights into the thermodynamic behavior of QDs, with significant implications for advancing research in nanotechnology and nanoenergy.

2. Methodology

The Debye T^3 model [15, 16] for heat capacity assumes that phonon propagation in bulk solids is continuous, isotropic, and unconfined. This assumption leads to a linear dispersion relation for phonons in bulk solids:

$$\omega(k) = v_s k \quad (1)$$

where ω is the angular frequency, k is the wave vector, and v_s is the speed of sound. Under this model, the number of phonon modes $n(\omega)$ and the phonon density of states $D(\omega)$ are expressed as:

$$n(\omega) = \frac{V\omega^3}{6\pi^2 v_s^3} \quad (2)$$

$$D(\omega) = \frac{d}{d\omega} n(\omega) = \frac{V\omega^2}{2\pi^2 v_s^3} \quad (3)$$

where V is the volume of the bulk material. The molar heat capacity at constant volume for bulk solids, derived from the Debye model, is given by:

$$C_V^{\text{molar}} = 9R \left(\frac{T}{T_D} \right)^3 \int_0^{T_D/T} \frac{x^4 e^x}{(e^x - 1)^2} dx \quad (4)$$

This is known as the Debye T^3 model, where R is the gas constant, T_D is the Debye temperature, and x is an integration variable related to the system's energy and temperature $x = \hbar\omega/k_B T$, \hbar is the reduced Planck constant, k_B is the Boltzmann constant. The mass-specific heat capacity can be expressed as:

$$C_V^m = \frac{C_V^{\text{molar}}}{M} = 9 \frac{R}{M} \left(\frac{T}{T_D} \right)^3 \int_0^{T_D/T} \frac{x^4 e^x}{(e^x - 1)^2} dx \quad (5)$$

where M is the molar mass.

The characteristic Debye temperature T_D is related to the Debye frequency ω_D by:

$$T_D = \frac{\hbar\omega_D}{k_B} = \frac{\hbar v_s}{k_B} \left(\frac{18\pi^2 N}{V} \right)^{1/3} \quad (6)$$

where N is the number of atoms.

Roslee et al. [14, 17] demonstrated that phonons in QDs do not propagate continuously due to quantum confinement effects, as illustrated in Fig. 1. These effects restrict phonon propagation to the dimensions of individual QDs, resulting in a modified dispersion relation based on the PIAB framework:

$$\omega(k) = \frac{\hbar k^2}{2m} \quad (7)$$

where m is the mass of an individual QD, and the wave numbers are discrete: $k = n\pi/L$, $n = 1, 2, 3, \dots$

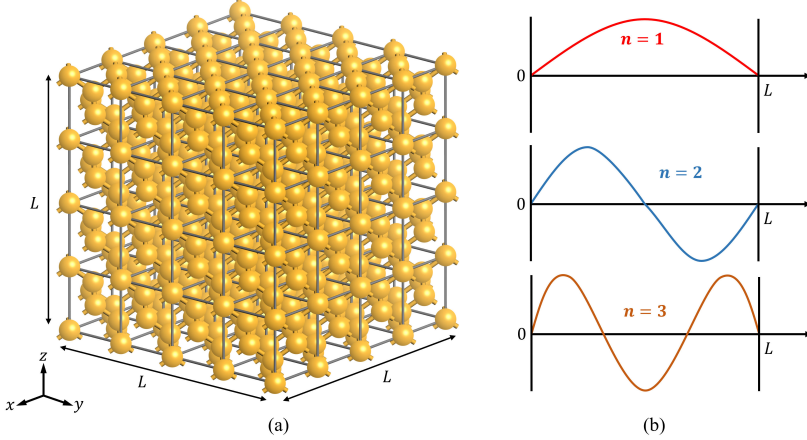


Figure 1: (a) Structure of the quantum dot. (b) Particle-in-a-box model.

The number of phonon modes $n(\omega)$ and the phonon density of states $D(\omega)$ for QDs are given by:

$$n(\omega) = \frac{V}{6\pi^2} \left(\frac{2m\omega}{\hbar} \right)^{3/2} \quad (8)$$

$$D(\omega) = \frac{d}{d\omega} n(\omega) = \frac{V}{\pi^2} \left(\frac{m^3 \omega}{2\hbar^3} \right)^{1/2} \quad (9)$$

where V now represents the quantum confinement volume of the QD.

The heat capacity for QDs, known as the PIAB $T^{3/2}$ model, is derived as:

$$C_V = \frac{3(3N - 6)}{2} k_B \left(\frac{T}{T_D} \right)^{3/2} \int_0^{T_D/T} \frac{x^{5/2} e^x}{(e^x - 1)^2} dx \quad (10)$$

The mass-specific heat capacity is:

$$C_V^m = \frac{3(3N - 6)}{2\rho V} k_B \left(\frac{T}{T_D} \right)^{3/2} \int_0^{T_D/T} \frac{x^{5/2} e^x}{(e^x - 1)^2} dx \quad (11)$$

where ρ is the material density.

The characteristic temperature T_D for the PIAB $T^{3/2}$ model can be related to the Debye frequency ω_D by:

$$T_D = \frac{\hbar\omega_D}{k_B} = \frac{\hbar^2}{2mk_B} \left(\frac{6\pi^2(3N - 6)}{V} \right)^{2/3} \quad (12)$$

Temperature is a statistical average typically applied to macroscopic systems containing a large number of particles. In such systems, the vast number of particles allows for an accurate statistical determination of temperature, and temperature fluctuations are negligible. However, at the nanoscale, where the number of particles is significantly reduced (to tens or hundreds), temperature fluctuations become more pronounced. This reduction poses challenges in obtaining sufficient statistical samples to mitigate these fluctuations. Under such conditions, the system may not achieve thermal equilibrium as assumed in traditional thermodynamics, complicating the precise determination of temperature.

Additionally, the reduced heat capacity at the nanoscale makes systems more sensitive to energy input changes, causing significant temperature fluctuations even with minimal energy variations. In small volumes, low heat capacity leads to increased temperature fluctuations, potentially obscuring the true thermodynamic behavior of the system. This limitation underscores the constraints of classical thermodynamics in small-scale systems. Temperature fluctuations can be described by the following relation [4]:

$$\langle (\Delta T)^2 \rangle = \frac{k_B T^2}{C_V} = \frac{k_B T^2}{\rho C_V^m V} \quad (13)$$

Here, the focus is on fluctuations as a function of volume. For temperature fluctuations to be negligible, the system's heat capacity must be sufficiently

large. However, at the nanoscale, the limited number of particles often results in a small heat capacity, leading to significant temperature fluctuations and questioning the applicability of traditional thermodynamic concepts.

For the quantitative analysis of temperature fluctuations, the normalized temperature fluctuation η_T is defined as:

$$\eta_T = \frac{\sqrt{\langle(\Delta T)^2\rangle}}{T} \quad (14)$$

where $\sqrt{\langle(\Delta T)^2\rangle}$ denotes the root-mean-square temperature fluctuation, and T represents the system's average temperature. The parameter η_T measures the relative magnitude of temperature fluctuations compared to the system's average temperature. When $\eta_T \ll 1$, temperature fluctuations are negligible relative to the average temperature, making it appropriate to describe the system using macroscopic thermodynamic variables such as temperature. In contrast, if $\eta_T \sim 1$ or larger, the fluctuations become comparable to or exceed the average temperature, challenging the validity of temperature as a well-defined and measurable quantity.

3. Results and discussion

The Debye T^3 model suggests that at low temperatures, the heat capacity of a system is proportional to T^3 . As the temperature approaches absolute zero, the heat capacity decreases sharply. According to thermal fluctuation theory, the amplitude of temperature fluctuations is inversely related to heat capacity. Thus, if the heat capacity decreases more rapidly than T^2 , as predicted by the Debye model, temperature fluctuations will diverge. However, this divergence does not accurately represent the behavior of physical systems, as quantum effects become significant at extremely low temperatures.

In contrast, the PIAB $T^{3/2}$ model predicts that at low temperatures, the heat capacity is proportional to $T^{3/2}$. This implies that the decrease in heat capacity is slower than T^2 , ensuring that temperature fluctuations do not diverge but instead converge. This behavior is strongly influenced by quantum effects, which dominate at very low temperatures and lead to deviations from classical predictions.

In this study, we calculated the heat capacity and temperature fluctuations for germanium, silicon, and diamond QDs using the Debye T^3 model and the PIAB $T^{3/2}$ model, as shown in Fig. 2.

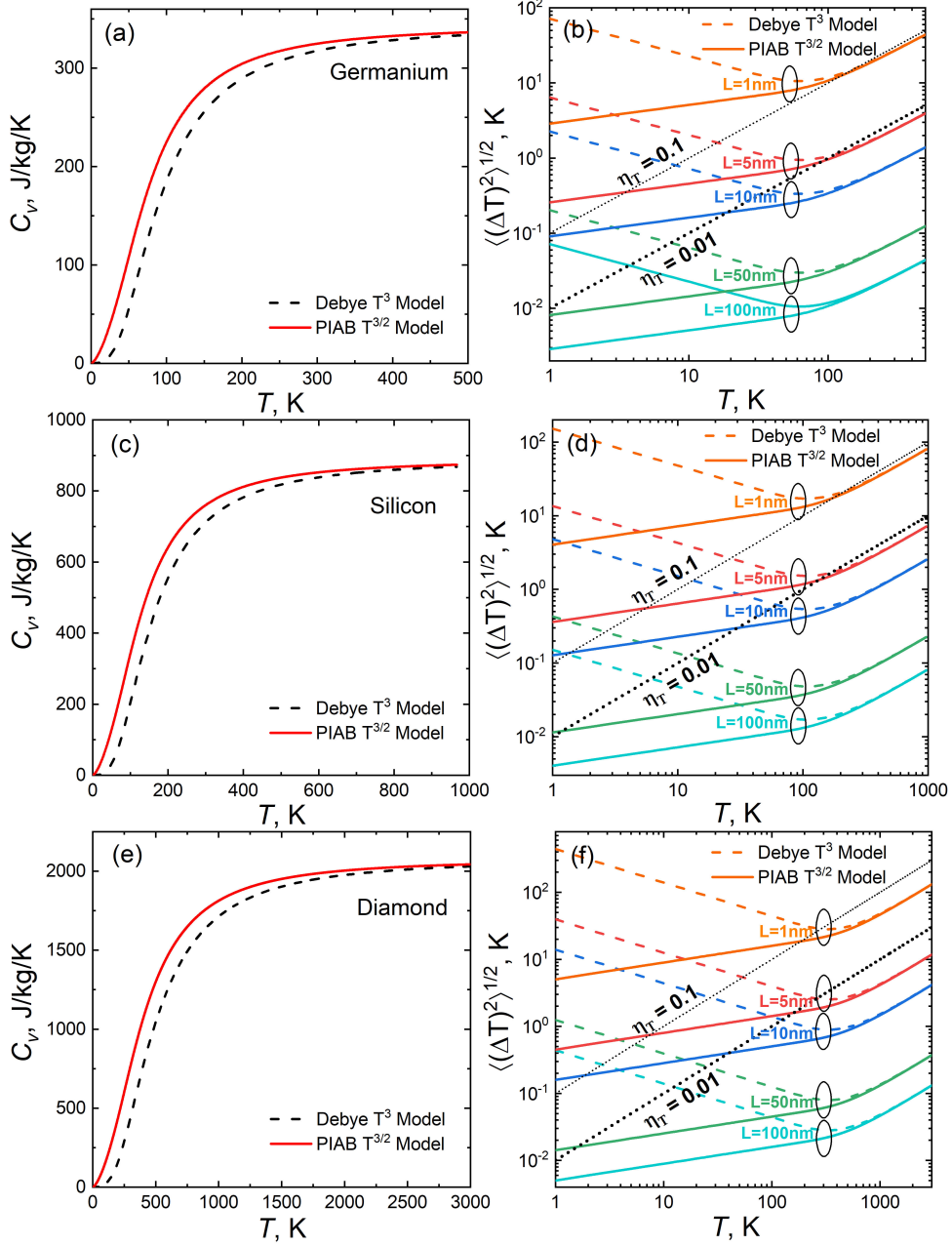


Figure 2: Heat capacity and temperature fluctuations as a function of temperature

For germanium, silicon, and diamond, the specific heat capacities calculated using the two models agree well at high temperatures, aligning with the Dulong-Petit law, which assumes full phonon excitation. At low temperatures, a notable difference arises: the heat capacity in the Debye model exhibits a T^3 dependence, while in the PIAB model, it follows a $T^{3/2}$ dependence. As shown in Fig. 2a, 2c, and 2e, the results of the PIAB $T^{3/2}$ model are slightly higher than those of the Debye T^3 model.

As predicted, the temperature fluctuations based on the Debye T^3 model tend to diverge at low temperatures. In contrast, the PIAB $T^{3/2}$ model provides convergent results, where temperature fluctuations decrease with decreasing temperature, as shown in Fig. 2b, 2d, and 2f. However, temperature fluctuations increase with decreasing size, highlighting the challenges in accurately defining temperature at the nanoscale and the associated limitations in defining other thermophysical properties.

How small must the temperature fluctuation be for temperature and thermodynamics to be considered meaningful? Typically, $\eta_T \leq 0.1$ or even $\eta_T \leq 0.01$ is used as the criterion. The errors and applicability of these two standards differ. These thresholds are illustrated in Fig. 2b, 2d, and 2f: if η_T exceeds the $\eta_T = 0.1$ line, the definition of temperature is deemed invalid; if η_T lies between the $\eta_T = 0.1$ and $\eta_T = 0.01$ lines, the definition of temperature is considered acceptable, albeit with significant errors; and if η_T is below the $\eta_T = 0.01$ line, the temperature definition is valid, and thermodynamic theory can be reliably applied.

The baseline and the temperature fluctuation curve intersect at a specific point, corresponding to a temperature. This implies that if the baseline is used as the judgment criterion, the temperature cannot be defined for values below this temperature, while the definition of temperature is valid for values above it. This temperature is referred to as the minimum allowed temperature. Based on different criteria ($\eta_T < 0.1$ and $\eta_T < 0.01$), we determined the minimum allowed temperatures for various sizes and listed them in Table 1.

When $\eta_T \leq 0.1$ is used as the criterion, the minimum allowed temperature for the three QDs at a length of 1 nm is less than 300 K. This indicates that, at room temperature, the temperature fluctuation of QDs with a length greater than 1 nm is less than 10% of the temperature itself. If this level of error is deemed acceptable, the definition of temperature can be considered valid.

When $\eta_T \leq 0.01$ is used as a stricter criterion, the minimum allowed temperature for the three QDs is less than 300 K when their length exceeds

Length	1nm	3nm	5nm	10nm	30nm	100nm
Minimum Allowed Temperature (K), $\eta \leq 0.1$						
Ge	126.8	9.8	3.6	0.7	0	0
Si	176.1	15.4	5.6	1.5	0	0
Diamond	186.1	20.7	7.5	1.9	0	0
Minimum Allowed Temperature (K), $\eta \leq 0.01$						
Ge	32347.7	15165.1	90.0	18.9	2.1	0
Si	55098.7	23695.0	134.2	29.9	3.4	0
Diamond	150653.7	589.8	160.2	40.0	4.5	0

Table 1: Minimum allowed temperatures for different QD lengths under conditions $\eta_T \leq 0.1$ and $\eta_T \leq 0.01$.

5 nm. This indicates that, at room temperature, the temperature fluctuation of QDs with a length greater than 5 nm is less than 1% of the temperature itself, meaning the temperature definition is highly accurate. Additionally, when the length reaches 100 nm, the minimum allowed temperature is 0, implying that temperature can be accurately defined at all values, and the fundamental assumptions of thermodynamics are valid at this scale.

For a more comprehensive analysis, the normalized temperature fluctuations as a function of size and temperature are plotted, as shown in Fig. 3. It is immediately apparent that the yellow region in the lower left corner of each image corresponds to $\eta_T > 1$, indicating that the temperature fluctuation exceeds the temperature itself. This implies that, at low temperatures and small sizes, the fundamental framework of thermodynamics breaks down entirely.

The dark blue region in the upper right corner of each image corresponds to $\eta_T \leq 0.1$, indicating that the temperature fluctuation is significantly smaller than the temperature itself. This implies that, at high temperatures and large sizes, the fundamental framework of thermodynamics is fully established. The equal normalized fluctuation lines $\eta_T = 0.1$ and $\eta_T = 0.01$ are also shown in the figure as reference lines. According to these standards, regions above and to the right of these lines are considered to have an accurate temperature definition, while regions below and to the left are considered to have an inaccurate temperature definition.

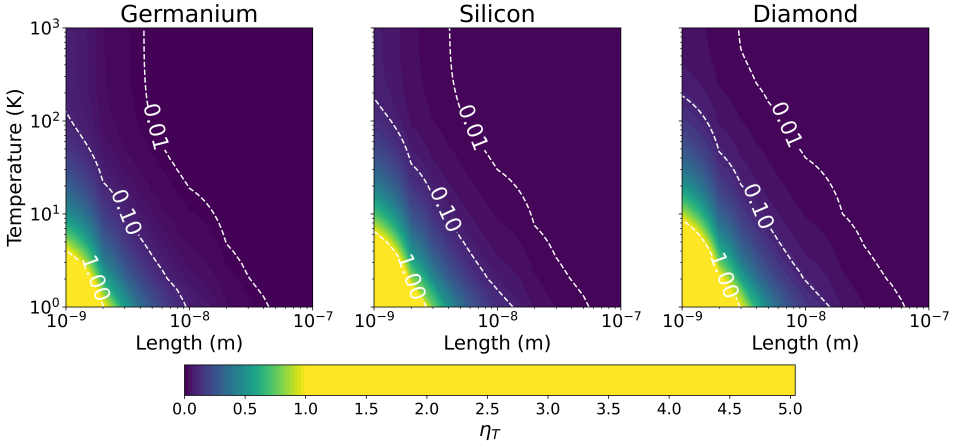


Figure 3: The normalized temperature fluctuations as a function of Length of QD and temperature

4. Conclusion

In this study, we conducted a pioneering analysis of temperature fluctuations in germanium, silicon, and diamond QDs, examining how these fluctuations depend on both temperature and size. For the first time, we established the minimum allowed value for the definition of temperature in QDs as a function of size and material, shedding light on the boundaries within which thermodynamic principles can be reliably applied at the nanoscale.

Our findings revealed that for QDs smaller than 5 nm, temperature fluctuations become so significant that they undermine the validity of the temperature concept, challenging conventional thermodynamic models. This indicates that at these small scales, quantum effects dominate and must be accounted for to accurately describe the system's thermal behavior. In contrast, for QDs with lengths greater than 100 nm, the minimum allowed temperature decreases to levels where temperature fluctuations are minimal, confirming that classical thermodynamic definitions remain applicable.

Funding

This work was supported by the China Scholarship Council (Grant No. 202308090243).

CRediT authorship contribution statement

Shixian Liu: Methodology, Validation, Formal analysis, Investigation, Writing - original draft, Writing - review & editing. **Vladimir I. Khvesyuk:** Conceptualization, Methodology, Supervision, Writing - review & editing.

Declaration of Competing Interest

The authors declare that they have no known competing financial interests or personal relationships that could have appeared to influence the work reported in this paper.

Acknowledgements

S. Liu gratefully acknowledges financial support from the China Scholarship Council.

Appendix A. Phonon Density of States

The phonon density of states $D(k)$ (or $D(\omega)$) for a three-dimensional solid can be determined by calculating the volume of a single state in k -space, V_{state} :

$$V_{\text{state}} = \Delta k_x \Delta k_y \Delta k_z = \left(\frac{2\pi}{L_x} \right) \left(\frac{2\pi}{L_y} \right) \left(\frac{2\pi}{L_z} \right) = \frac{8\pi^3}{L_x L_y L_z} = \frac{8\pi^3}{V}, \quad (\text{A.1})$$

where $V = L_x L_y L_z$ is the volume of the solid. The total volume of k -space for all states is enclosed in a sphere with volume V_{total} :

$$V_{\text{total}} = \frac{4}{3}\pi k^3. \quad (\text{A.2})$$

The number of states $n(k)$ with wave vectors smaller than k is given by:

$$n(k) = \frac{V_{\text{total}}}{V_{\text{state}}} = \frac{\frac{4}{3}\pi k^3}{\frac{8\pi^3}{V}} = \frac{V k^3}{6\pi^2}. \quad (\text{A.3})$$

The phonon density of states $D(k)$ is defined as the number of modes $n(k)$ per unit wave vector:

$$D(k) = \frac{d}{dk} n(k) = \frac{V k^2}{2\pi^2}. \quad (\text{A.4})$$

Appendix A.1. Debye T^3 Model

With a linear dispersion relation, $n(\omega)$ can be expressed as:

$$n(\omega) = \frac{V}{6\pi^2} \left(\frac{\omega}{v_s} \right)^3. \quad (\text{A.5})$$

The phonon density of states $D(\omega)$ becomes:

$$D(\omega) = \frac{d}{d\omega} n(\omega) = \frac{V\omega^2}{2\pi^2 v_s^3}. \quad (\text{A.6})$$

Appendix A.2. PIAB $T^{3/2}$ Model

For a quadratic dispersion relation, $n(\omega)$ is given by:

$$n(\omega) = \frac{V}{6\pi^2} \left(\frac{2m\omega}{\hbar} \right)^{3/2}. \quad (\text{A.7})$$

The corresponding phonon density of states is:

$$D(\omega) = \frac{d}{d\omega} n(\omega) = \frac{V}{\pi^2} \left(\frac{m^3 \omega}{2\hbar^3} \right)^{1/2}. \quad (\text{A.8})$$

Appendix B. Heat Capacity

The thermal energy U can be expressed as:

$$U = \int_0^{\omega_D} \left(\frac{1}{2} + \frac{1}{e^{\frac{\hbar\omega}{k_B T}} - 1} \right) \hbar\omega D(\omega) d\omega. \quad (\text{B.1})$$

The heat capacity at constant volume C_v is:

$$C_v = \frac{dU}{dT} = \int_0^{\omega_D} \frac{d}{dT} \left(\frac{1}{e^{\frac{\hbar\omega}{k_B T}} - 1} \right) \hbar\omega D(\omega) d\omega. \quad (\text{B.2})$$

Appendix B.1. Debye T^3 Model

The Debye wave vector k_D satisfies:

$$n(k_D) = \frac{V k_D^3}{6\pi^2} = 3N. \quad (\text{B.3})$$

The Debye frequency ω_D can be written as:

$$\omega_D = v_s \cdot k_D = v_s \left(\frac{6\pi^2 \cdot 3N}{V} \right)^{1/3}. \quad (\text{B.4})$$

Substituting $D(\omega)$ into U gives:

$$U = \int_0^{\omega_D} \left(\frac{1}{2} + \frac{1}{e^{\frac{\hbar\omega}{k_B T}} - 1} \right) \hbar\omega \frac{V\omega^2}{2\pi^2 v_s^3} d\omega. \quad (\text{B.5})$$

Introducing $x = \frac{\hbar\omega}{k_B T}$ and $T_D = \frac{\hbar\omega_D}{k_B}$, we have:

$$U = 9Nk_B T \left(\frac{T}{T_D} \right)^3 \int_0^{T_D/T} \left(\frac{1}{2} + \frac{1}{e^x - 1} \right) x^3 dx. \quad (\text{B.6})$$

The heat capacity becomes:

$$C_V = \frac{dU}{dT} = 9Nk_B \left(\frac{T}{T_D} \right)^3 \int_0^{T_D/T} \frac{x^4 e^x}{(e^x - 1)^2} dx, \quad (\text{B.7})$$

where N is the number of atoms.

The molar heat capacity is:

$$C_{V,\text{molar}} = 9R \left(\frac{T}{T_D} \right)^3 \int_0^{T_D/T} \frac{x^4 e^x}{(e^x - 1)^2} dx, \quad (\text{B.8})$$

with $R = k_B N_A$, where N_A is Avogadro's number.

Appendix B.2. PIAB $T^{3/2}$ Model

In QDs, the vibrational degrees of freedom are represented by $3N - 6$, where the subtraction accounts for the removal of three translational and three rotational degrees of freedom. The relationship between the vibrational degrees of freedom and the maximum wave vector k_D is given by:

$$n(k_D) = \frac{V k_D^3}{6\pi^2} = F = 3N - 6. \quad (\text{B.9})$$

The maximum frequency ω_D can be expressed as:

$$\omega_D = \frac{\hbar}{2m} k_D = \frac{\hbar}{2m} \left(\frac{6\pi^2 \cdot F}{V} \right)^{1/3}. \quad (\text{B.10})$$

The thermal energy becomes:

$$U = \int_0^{\omega_D} \left(\frac{1}{2} + \frac{1}{e^{\frac{\hbar\omega}{k_B T}} - 1} \right) \hbar\omega \frac{V}{\pi^2} \left(\frac{m^3 \omega}{2\hbar^3} \right)^{1/2} d\omega. \quad (\text{B.11})$$

With $x = \frac{\hbar\omega}{k_B T}$ and $T_D = \frac{\hbar\omega_D}{k_B}$:

$$T_D = \frac{\hbar^2}{2mk_B} \left(\frac{6\pi^2 \cdot F}{V} \right)^{2/3}, \quad (\text{B.12})$$

$$T_D^{3/2} = \left(\frac{\hbar^2}{2mk_B} \right)^{3/2} \frac{6\pi^2 \cdot F}{V}. \quad (\text{B.13})$$

The thermal energy expression becomes:

$$U = \frac{3(3N - 6)}{2} k_B T \left(\frac{T}{T_D} \right)^{3/2} \int_0^{T_D/T} \left(\frac{1}{2} + \frac{1}{e^x - 1} \right) x^{3/2} dx. \quad (\text{B.14})$$

The heat capacity is:

$$C_v = \frac{3(3N - 6)}{2} k_B \left(\frac{T}{T_D} \right)^{3/2} \int_0^{T_D/T} \frac{x^{5/2} e^x}{(e^x - 1)^2} dx, \quad (\text{B.15})$$

where N is the number of atoms.

References

- [1] G. David L., States of matter, Dover Publications, Mineola, New York, 1985.
- [2] G. Michel, D. J. Searles, Local Fluctuation Theorem for Large Systems, Phys. Rev. Lett. 110 (26) (2013) 260602. doi:10.1103/PhysRevLett.110.260602.

- [3] G. Chen, Non-Fourier phonon heat conduction at the microscale and nanoscale, *Nat Rev Phys* 3 (8) (2021) 555–569. doi:10.1038/s42254-021-00334-1.
- [4] L. D. Landau, E. M. Lifshitz, *Statistical Physics: Volume 5*, Elsevier, 2013.
- [5] T. C. P. Chui, D. R. Swanson, M. J. Adriaans, J. A. Nissen, J. A. Lipa, Temperature fluctuations in the canonical ensemble, *Phys. Rev. Lett.* 69 (21) (1992) 3005–3008. doi:10.1103/PhysRevLett.69.3005.
- [6] M. Hartmann, G. Mahler, O. Hess, Local versus global thermal states: Correlations and the existence of local temperatures, *Phys. Rev. E* 70 (6) (2004) 066148. doi:10.1103/PhysRevE.70.066148.
- [7] M. Hartmann, G. Mahler, O. Hess, Existence of Temperature on the Nanoscale, *Phys. Rev. Lett.* 93 (8) (2004) 080402. doi:10.1103/PhysRevLett.93.080402.
- [8] G. M. Wang, E. M. Sevick, E. Mittag, D. J. Searles, D. J. Evans, Experimental Demonstration of Violations of the Second Law of Thermodynamics for Small Systems and Short Time Scales, *Phys. Rev. Lett.* 89 (5) (2002) 050601. doi:10.1103/PhysRevLett.89.050601.
- [9] Q. Cheng, S. Rajauria, E. Schreck, R. Smith, N. Wang, J. Reiner, Q. Dai, D. Bogy, Precise nanoscale temperature mapping in operational micro-electronic devices by use of a phase change material, *Sci Rep* 10 (1) (2020) 20087. doi:10.1038/s41598-020-77021-1.
- [10] X. Lin, M. Kong, N. Wu, Y. Gu, X. Qiu, X. Chen, Z. Li, W. Feng, F. Li, Measurement of Temperature Distribution at the Nanoscale with Luminescent Probes Based on Lanthanide Nanoparticles and Quantum Dots, *ACS Appl. Mater. Interfaces* 12 (47) (2020) 52393–52401. doi:10.1021/acsami.0c15697.
- [11] A. Chmielewski, C. Ricolleau, D. Alloyeau, G. Wang, J. Nelayah, Nanoscale temperature measurement during temperature controlled *in situ* TEM using Al plasmon nanothermometry, *Ultramicroscopy* 209 (2020) 112881. doi:10.1016/j.ultramic.2019.112881.

- [12] V. Novotny, P. Meincke, J. Watson, Effect of size and surface on the specific heat of small lead particles, *Physical Review Letters* 28 (14) (1972) 901.
- [13] A. J. McNamara, B. J. Lee, Z. M. Zhang, Quantum Size Effect on the Lattice Specific Heat of Nanostructures, *Nanoscale and Microscale Thermophysical Engineering* 14 (1) (2010) 1–20. doi:10.1080/15567260903468612.
- [14] A. E. Roslee, S. K. Muzakir, J. Ismail, M. M. Yusoff, R. Jose, A heat capacity model of $T^{3/2}$ dependence for quantum dots, *Phys. Chem. Chem. Phys.* 19 (1) (2017) 408–418. doi:10.1039/C6CP07173B.
- [15] Z. M. Zhang, *Nano/Microscale Heat Transfer*, Mechanical Engineering Series, Springer International Publishing, Cham, 2020. doi:10.1007/978-3-030-45039-7.
- [16] G. P. Srivastava, *The Physics of Phonons*, 2nd Edition, CRC Press, Boca Raton, 2022. doi:10.1201/9781003141273.
- [17] A. E. Roslee, N. A. Nik Mohamed, P. Thamburaja, R. Jose, A generalized thermophysical model for materials from molecular clusters to bulk crystals, *Physica B: Condensed Matter* 659 (2023) 414877. doi:10.1016/j.physb.2023.414877.